Table 1 (*Continued*)

Peak	Observed mass (theoretical mass[a])	Structure[b]	Abbreviation
k	2197.2 (2197.8)	NeuAc α2→3Gal β1→4GlcNAc β1→2Man α1↘6 Fuc α1↘6 Gal β1→4GlcNAc β1→2Man α1↗3 Man β1→4GlcNAc β1→4GlcNAc Gal β1→4GlcNAc β1→2Man α1↘6 Fuc α1↘6 NeuAc α2→3Gal β1→4GlcNAc β1→2Man α1↗3 Man β1→4GlcNAc β1→4GlcNAc	G2S1
l	2156.1 (2156.8)	Man α1↘6 Man α1↗3 Man α1↘6 Fuc α1↘6 NeuAc α2→3Gal β1→4GlcNAc β1→2Man α1↗3 Man β1→4GlcNAc β1→4GlcNAc	HybridS1
m	2488.2 (2488.9)	NeuAc α2→3Gal β1→4GlcNAc β1→2Man α1↘6 Fuc α1↘6 NeuAc α2→3Gal β1→4GlcNAc β1→2Man α1↗3 Man β1→4GlcNAc β1→4GlcNAc	G2S2

[a] Theoretical masses are of 2-AA labeled oligosaccharides, calculated as monoisotopic mass of $[M-H]^-$.
[b] Linkage positions are tentatively assigned. All structures are derivatized with 2-AA at the reducing ends.

tion. After sialidase digestion of fraction **j**, the bigger left peak moved to G1, smaller right peak moved to G1′ (data not shown). From these data, we could assign the peaks due to G1S1 and G1′S1 (Table 1) by CE.

After sialylated species were observed, high-mannose type oligosaccharides (M5 to M9) were migrated in this order (Fig. 6).

GN1G0 was also included in this region. The IgG molecules having these high-mannose type oligosaccharides are assumed to be secreted from cultured cells after incomplete processing of biosynthesis as reported previously [35]. In the biosynthetic pathway of *N*-linked oligosaccharides in mammalian cells, initial form of glycosylation in protein is $Glc_3Man_9GlcNAc_2$-Asn. The oligosaccharide is trimmed to $Man_9GlcNAc_2$ (M9) by glucosidase I and II, and then further trimmed by mannosidase from $Man_8GlcNAc_2$ (M8) to yield $Man_5GlcNAc_2$ (M5). Then, GlcNAc residue is transferred to mannose of trimannosyl core by GlcNAc-transferase I, resulting in hybrid type oligosaccharide. After continuous digestion of two mannose residues, a Fuc residue is transferred to core GlcNAc, yielding a complex

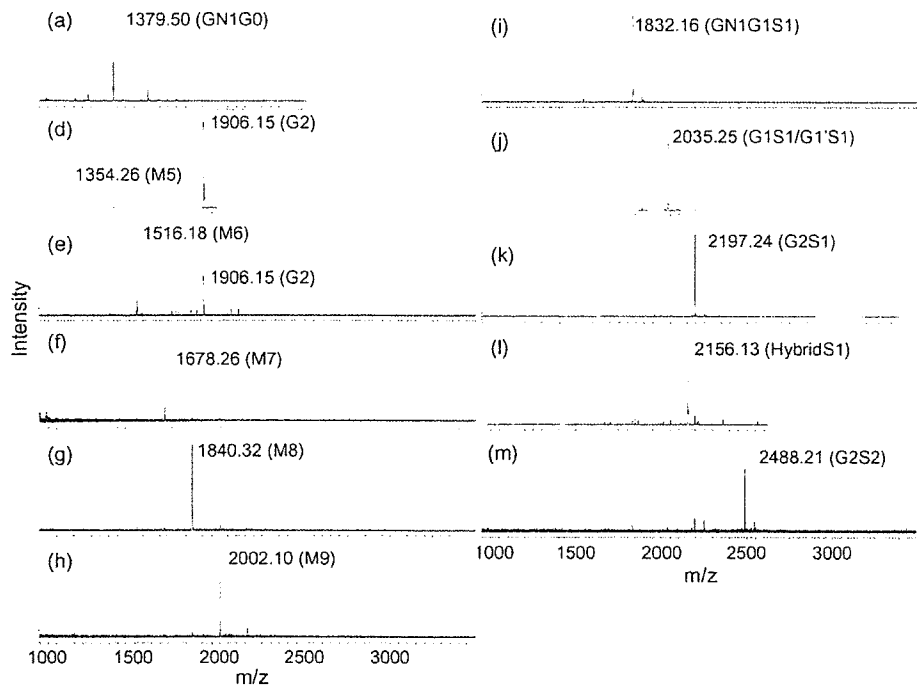

Fig. 4. MALDI-TOF mass spectra of 2-AA labeled oligosaccharides from rituximab. Peaks **a**, **d–m** are indicated in Fig. 3. Mass spectra were observed in negative/reflector mode using DHB as matrix as described in Section 2. Abbreviation of oligosaccharide structures and observed masses (monoisotopic mass) are also shown. The list of oligosaccharides is shown in Table 1.

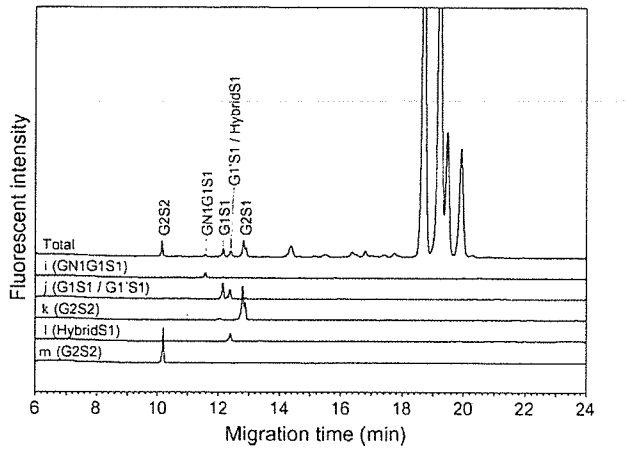

Fig. 5. Peak assignment of sialic acid-containing oligosaccharides of rituximab. Total mixture of oligosaccharides from rituximab was analyzed by CE-LIF (total). The same sample was separated by HPLC (Fig. 2, **a**, **d–i**) and the collected peaks determined by MALDI-TOF-MS (Fig. 4) were analyzed by CE. Assigned structures are shown on the peaks as abbreviations (Table 1). The analytical conditions of CE were described in Fig. 2.

type GN1G0. Further processing by a series of glycosyltransferases occurs in the Golgi compartments, and finally completely processed complex type oligosaccharides are synthesized [36]. However, it is accepted that individual glycosylation reaction does not always proceed to completion, leading to the secretion of incompletely processed high-mannose type, hybrid type oligosaccharides as minor oligosaccharides [34,35,37]. These observations support that high-mannose type and hybrid type oligosaccharides were detected as minor oligosaccharide species in the case of rmAb produced by CHO cell line.

After these incompletely processed-species (IP), major oligosaccharides (G0, G1, G1′ and G2) which are previously reported as typical oligosaccharides in rmAb, were observed from 18.2 to 20 min.

The results indicate that the *N*-linked oligosaccharides of mAb show high heterogeneity in minor oligosaccharides and the

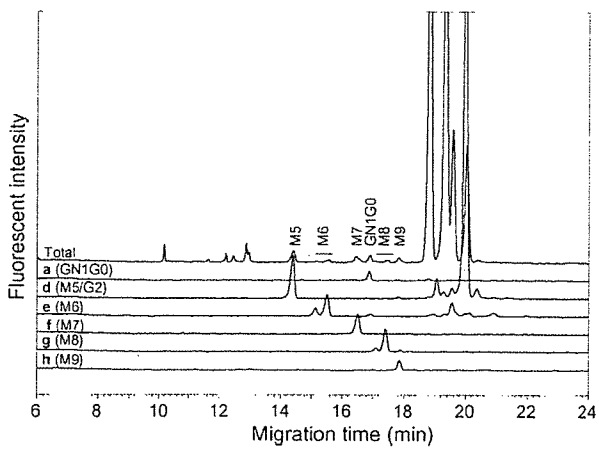

Fig. 6. Peak assignment of asialo- and high-mannose type oligosaccharides of rituximab. Sialic acid-containing oligosaccharides were assigned in the same manner as described in Fig. 5.

Table 2
Precision in oligosaccharide profiling of rituximab

Preparation	Corrected area (%)							
	S2	S1	M5-M9	GN1G0	G0	G1	G1′	G2
1	0.9	2.7	4.0	0.6	38.0	34.2	10.1	9.6
2	1.0	2.6	4.1	0.6	38.2	34.2	10.0	9.4
3	0.9	3.0	3.9	0.6	37.9	34.2	10.1	9.4
Average	0.9	2.8	4.0	0.6	38.0	34.2	10.1	9.5
SD	0.1	0.2	0.1	0.0	0.2	0.0	0.1	0.1
RSD (%)	6.2	7.5	2.5	0.0	0.4	0.0	0.6	1.2

Three preparations of 2-AA labeled *N*-linked oligosaccharides from rituximab were analyzed by CE-LIF.

present CE-LIF method for profiling of *N*-linked oligosaccharide using 2-AA labeling has high resolving ability to separate these oligosaccharides. In contrast, HPLC method using amino-column requires much longer time, and cannot separate of M5 and G2.

3.4. Quantitative evaluation and analysis of other rmAb pharmaceuticals

We evaluated the precision reproducibility of relative distribution of oligosaccharides including S2, S1, high-mannose type oligosaccharides using the present technique by repeated analysis of rituximab. Three preparations of 2-AA labeled oligosaccharides from a sample of rituximab were analyzed on CE-LIF. The result is summarized in Table 2.

Good reproducibility with the RSD of relative corrected peak areas of less than 7.5% (SD were 0.2% or below) was shown even in the analysis of minor oligosaccharides such as S2 and S1. As for major oligosaccharides (G0, G1, G1′ and G2), the RSD showed excellent values, and were 0.4, 0.0, 0.6 and 1.2%, respectively.

Based on the results on precision analysis, we applied the present method to the *N*-linked oligosaccharide profiling of some rmAb pharmaceuticals, rituximab, trastuzumab and palivizumab (Fig. 7).

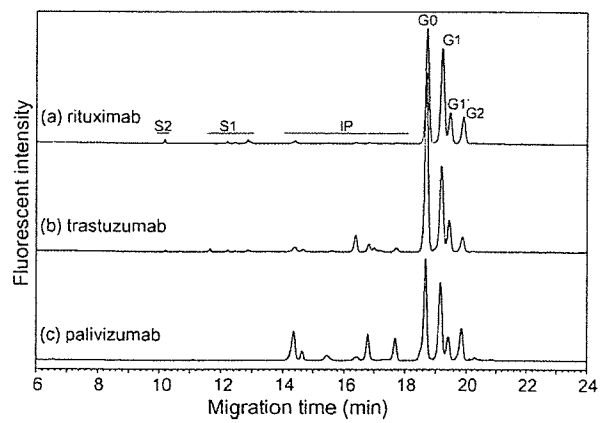

Fig. 7. Comparison of *N*-linked oligosaccharide profile from some rmAb pharmaceuticals by CE-LIF after 2-AA derivatization. The conditions of CE-LIF analysis were as in Fig. 2.

All three preparations included G0, G1, G1′ and G2 as major oligosaccharides. However, the profiles of minor oligosaccharides such as sialyl oligosaccharides (S2 and S1) and IP are specific to each preparation. In trastuzumab (Fig. 7b), S2 and S1 peaks are quite small but IP peaks are more abundant than those of rituximab. The data observed in these two rmAb preparations are well comparable with lot-analysis data reported previously [30]. Palivizumab showed characteristic profiles, and large amount of IP was observed. In contrast, there were no peaks in the region of S2 and S1.

The present method can monitor the processing of oligosaccharides in rmAb samples. For example, rituximab contains minute amount of high-mannose type oligosaccharides, indicating processing is nearly complete but palivizumab contains a large amount of IP. Difference of the amount of sialyl- and high-mannose type oligosaccharides in rmAb possibly affects clearance or biological activity of the pharmaceutical preparations [31–33]. Moreover, high-mannose structures are likely to influence the effector functions of the antibody and may alter the structure of the Fc region [38]. It has been demonstrated that the proportion of high-mannose type oligosaccharides increase during cell culture [39]. Cell culture under low glutamine or glucose concentration leads to increase hybrid type and high-mannose type oligosaccharides [34]. Therefore, it is important to evaluate these minor oligosaccharides for pharmaceutical development of rmAb. The present method will be a powerful tool to evaluate total *N*-linked oligosaccharides of rmAb pharmaceuticals for such purpose.

4. Conclusion

In this study, we developed CE-LIF method for high-resolution analysis of *N*-linked oligosaccharides from mAb pharmaceuticals, and assigned all peaks in the electropherogram using a combination of HPLC and MALDI-TOF-MS. In the model study using rituximab, we demonstrated that the present CE-LIF method could separate total *N*-linked oligosaccharides not only typical asialo-biantennary complex type but also minor sialo-complex type, high-mannose type and hybrid type oligosaccharides with high resolution and high reproducibility. Our results show that the present method is quite useful for rapid, quantitative and exhaustive evaluation of *N*-linked oligosaccharide profile of mAb pharmaceuticals in various development stages such as, for example, clone selection and bioprocess control, detailed characterization for approval application and lot release testing.

References

[1] A. Varki, R. Cummings, J. Esko, H. Freeze, G. Hart, J. Marth, Essentials of Glycobiology, Cold Spring Harbor Laboratory Press, New York, 1999.
[2] T. Muramatsu, Glycobiology 3 (1993) 291.
[3] M. Fukuda, Cancer Res. 56 (1996) 2237.
[4] J. Zara, R.K. Naz, Front. Biosci. 3 (1998) 1028.
[5] B.J. Sutton, D.C. Phillips, Biochem. Soc. Trans. 11 (1983) 130.
[6] T. Mizouchi, T. Taniguchi, A. Shimizu, A. Kobata, J. Immunol. 129 (1982) 2016.
[7] S. Fujii, T. Nishiura, A. Nishikawa, R. Miura, N. Taniguchi, J. Biol. Chem. 265 (1990) 6009.
[8] R.J. Ratherbarrow, N. Richardson, A. Feinstein, Mol. Immunol. 22 (1985) 407.
[9] M.H. Tao, S.L. Morrison, J. Immunol. 143 (1989) 2595.
[10] M.R. Walker, J. Lund, K.M. Thomsom, R. Jefferis, Biochem. J. 259 (1989) 347.
[11] K.A. Leader, B.M. Kumpel, A.G. Hadley, B.A. Bradley, Immunology 72 (1991) 481.
[12] P. Umana, J. Jean-Mairet, R. Moudry, H. Amstutz, J.E. Bailey, Nat. Biotechnol. 17 (1999) 176.
[13] J. Davies, L. Jiang, L.Z. Pan, M.J. LaBarre, D. Anderson, M. Reff, Biotechnol. Bioeng. 4 (2001) 288.
[14] R.L. Shields, J. Lai, R. Keck, L.Y. O'Connell, K. Hong, Y.G. Meng, S.H. Weikert, L.G. Presta, J. Biol. Chem. 277 (2002) 26733.
[15] T. Shinkawa, K. Nakamura, N. Yamane, E. Shoji-Hosaka, Y. Kanda, M. Sakurada, K. Uchida, H. Anazawa, M. Satoh, M. Yamasaki, N. Hanai, K. Shitara, J. Biol. Chem. 278 (2003) 3466.
[16] M.R. Hardy, R.R. Townsend, Y.C. Lee, Methods Enzymol. 179 (1989) 65.
[17] M. Spellman, Anal. Chem. 62 (1990) 1714.
[18] K.R. Anumula, Anal. Biochem. 220 (1994) 275.
[19] J.C. Bigge, T.P. Patel, J.A. Bruce, P.N. Goulding, S.M. Charles, B. Parekh, Anal. Biochem. 230 (1995) 229.
[20] K.R. Anumula, S.T. Dhume, Glycobiology 8 (1998) 685.
[21] M. Nakano, K. Kakehi, M.H. Tsai, Y.C. Lee, Glycobiology 14 (2004) 431.
[22] S. Kamoda, M. Nakano, R. Ishikawa, S. Suzuki, K. Kakehi, J. Proteome Res. 4 (2005) 146.
[23] R. Naka, S. Kamoda, A. Ishizuka, M. Kinoshita, K. Kakehi, J. Proteome Res. 5 (2006) 88.
[24] F.T. Chen, R.A. Evangelista, Electrophoresis 19 (1998) 2639.
[25] S. Ma, W. Nashabeh, Anal. Chem. 71 (1999) 5185.
[26] K. Kakehi, T. Funakubo, S. Suzuki, Y. Oda, Y. Kitada, J. Chromatogr. A 863 (1999) 205.
[27] T.S. Raju, Anal. Biochem. 283 (2000) 125.
[28] K. Nakajima, Y. Oda, M. Kinoshita, K. Kakehi, J. Proteome Res. 2 (2003) 81.
[29] S. Ma, W. Lau, R.G. Keck, J.B. Briggs, A.J. Jones, K. Moorhouse, W. Nashabeh, Methods Mol. Biol. 308 (2005) 397.
[30] S. Kamoda, C. Nomura, M. Kinoshita, S. Nishiura, R. Ishikawa, K. Kakehi, N. Kawasaki, T. Hayakawa, J. Chromatogr. A 1050 (2004) 211.
[31] V. Gross, K. Steube, T.-A. Tran-Thi, D. Haussinger, G. Legler, K. Decker, P.C. Heinrich, W. Gerok, Eur. J. Biochem. 162 (1987) 83.
[32] N. Jenkins, E.M. Curling, Enzyme Microb. Technol. 16 (1994) 354.
[33] A. Wright, S.L. Morrison, J. Exp. Med. 180 (1994) 1087.
[34] D.C.F. Wong, K.T.K. Wong, L.T. Goh, C.K. Heng, M.G.S. Yap, Biotechnol. Bioeng. 89 (2005) 164.
[35] M.J. Bailey, A.D. Hooker, C.S. Adams, S. Zhang, D.C. James, J. Chromatogr. B 826 (2005) 177.
[36] R. Kornfeld, S. Kornfeld, Annu. Rev. Biochem. 54 (1985) 631.
[37] A.D. Hooker, N.H. Green, A.J. Baines, A.T. Bull, N. Jenkins, P.G. Strange, D.C. James, Biotechnol. Bioeng. 63 (1999) 560.
[38] R. Jefferis, J. Lund, M. Goodall, Immunol. Lett. 44 (1995) 111.
[39] A.D. Hooker, M.H. Goldman, N.H. Markham, D.C. James, A.P. Ison, A.T. Bull, N. Jenkins, Biotechnol. Bioeng. 48 (1995) 639.

Available online at www.sciencedirect.com

ScienceDirect

Analytical Biochemistry 362 (2007) 245–257

ANALYTICAL BIOCHEMISTRY

www.elsevier.com/locate/yabio

Development of an apparatus for rapid release of oligosaccharides at the glycosaminoglycan–protein linkage region in chondroitin sulfate-type proteoglycans

Yu-ki Matsuno [a], Keita Yamada [a], Ayumi Tanabe [a], Mitsuhiro Kinoshita [a], Shu-zou Maruyama [b], Yu-suke Osaka [b], Takashi Masuko [a], Kazuaki Kakehi [a,*]

[a] *Faculty of Pharmaceutical Sciences, Kinki University, Kowakae 3-4-1, Higashi-osaka 577-8502, Japan*

[b] *Analytical and Measuring Instruments Division, Shimadzu Corp., Nishinokyo-kuwabaracho 1, Nakagyo-ku, Kyoto 604-8511, Japan*

Received 14 November 2006

Available online 20 December 2006

Abstract

An apparatus, AutoGlycoCutter (AGC), was developed as a tool for rapid release of *O*-linked-type glycans under alkaline conditions. This system allowed rapid release of oligosaccharides at the glycosaminoglycan–protein linkage region in proteoglycans (PGs). After digestion of PGs with chondroitinase ABC, the oligosaccharides at the linkage region were successfully released from the protein core by AGC within 3 min. The reducing ends of the released oligosaccharides were labeled with 2-aminobenzoic acid and analyzed by a combination of capillary electrophoresis (CE) and matrix-assisted laser desorption time-of-flight mass spectrometry. In addition, the unsaturated disaccharides produced by chondroitinase ABC derived from the outer parts of the glycans were labeled with 2-aminoacridone and analyzed by CE to determine the disaccharide compositions. We evaluated AGC as a method for structural analysis of glycosaminoglycans in some chondroitin-sulfate-type PGs (urinary trypsin inhibitor, bovine nasal cartilage PG, bovine aggrecan, bovine decorin, and bovine biglycan). Recoveries of the released oligosaccharides were 57–73% for all PGs tested in the present study. In particular, we emphasize that the use of AGC achieved ca. 1000-fold rapid release of *O*-glycans compared with the conventional method.

Keywords: Proteoglycan; In-line flow system; Capillary electrophoresis; Linkage region

Proteoglycans (PGs)[1] consist of a protein core substituted with glycosaminoglycan (GAG) chain(s) and are ubiquitously found in the extracellular matrix. PGs are associated with the cell surface of eucaryotic cells [1,2] and have been recognized as important molecules in development and connective tissue assembly [3,4]. PGs are also directly implicated in a large variety of human diseases. For instance, the significant change of PG content or structural alterations of GAGs in tumor states have been reported [5,6].

GAGs attached to PGs also perform a variety of biological functions based on the interactions with various proteins such as collagen and growth factors [7]. GAG chains are linear polymers composed of repeating disaccharides of hexosamine and hexuronic acid and are generally sulfated except for hyaluronic acid (HA), while keratan sulfate (KS) consists of a poly-*N*-acetyllactosamine backbone.

* Corresponding author. Fax: +81 6 6721 2353.
E-mail address: k_kakehi@phar.kindai.ac.jp (K. Kakehi).

[1] *Abbreviations used:* PGs, proteoglycans; GAG, glycosaminoglycan; HA, hyaluronic acid; KS, keratan sulfate; CS/DS, chondroitin/dermatan sulfate; HP/HS heparin/heparan sulfate; MALDI-TOF MS, matrix-assisted laser desorption ionization time-of-flight mass spectrometry; UTI urinary trypsin inhibitor; BNC, bovine nasal cartilage; 2AA, 2-aminobenzoic acid; AMAC, 2-aminoacridone; PEG, polyethyleneglycol; AGC, Autoglycocutter; DHB,2,5-dihydroxybenzoic acid; CE, capillary electrophoresis.

0003-2697/$ - see front matter © 2006 Elsevier Inc. All rights reserved.
doi:10.1016/j.ab.2006.12.027

GAGs except HA are covalently attached to serine residues of core protein in an *O*-linked manner through the core tetrasaccharide structure of GlcAβ1-3Galβ1-3Galβ1-4Xylβ1-*O*-Ser [8,9]. The linkage-region glycan is synthesized through stepwise sequential addition of each monosaccharide from the corresponding sugar nucleotide to a specific serine residue in a core protein. Chondroitin/dermatan sulfate (CS/DS) is synthesized once GalNAc is transferred to the common linkage region, while heparin/heparan sulfate (HP/HS) is formed if GlcNAc is first added. So far, a variety of linkage-region structures modified with various sulfation patterns have been identified in chondroitin sulfate PGs derived from many cartilages such as whale cartilage [10], bovine nasal septum cartilage [11,12], shark cartilage [13,14], and bovine articular cartilage [15,16]. Because the sulfation of Gal residues in the glycans at the linkage region has not been found in HP/HS–PGs [17,18], sulfated Gal structures are considered to play an important role in GAG biosynthesis, especially in the sorting mechanisms leading to CS/DS or to HP/HS. Phosphorylation at Xyl residue in the linkage region has also been found in some PGs [14,19,20]. Previous studies suggested that dephosphorylation took place soon after the transfer reaction of GlcA to the trisaccharide, Galβ1-3Galβ1-4Xyl [21,22], and *in vitro* enzyme assays using human glucuronyltransferase I demonstrated that this enzyme showed higher activity toward the phosphorylated acceptor substrate, Gal-Gal-Xyl(2-*O*-phosphate)-Ser [23].

From these observations, structural analysis of linkage-region oligosaccharides is important for elucidating the mechanism of GAG biosynthesis. To analyze the oligosaccharides at the linkage region, they are usually released from the core protein by β-elimination reaction in alkaline solution. The releasing reaction is usually performed under mild conditions for a long time (typically, 0.5 M LiOH at 4 °C for 15 h) to prevent degradation by peeling reaction or random cleavage [24]. Endo-β-xylosidase and cellulases that exhibit endo-β-xylosidase activity have been reported for releasing GAGs from the core protein [25,26], but specificity of the enzyme is a big problem for routine use.

So far, structural analysis of the oligosaccharides at the linkage region has been performed by various analytical methods such as high-performance liquid chromatography (HPLC), ^{1}H-NMR spectroscopy, and matrix-assisted laser desorption ionization time-of-flight mass spectrometry (MALDI-TOF MS). ^{1}H-NMR spectroscopy is a powerful technique for determination of oligosaccharide structure but usually requires large amounts of the sample (~mg). For sensitive analysis, nonreductive alkaline β-elimination followed by fluorescent labeling with 2-aminobenzamide was reported [24].

In the present study, we fabricated an apparatus for rapid release of GAGs from the core protein by using an in-line flow system and evaluated the method for the analysis of linkage oligosaccharides derived from five CS/DS–PGs.

Materials and methods

Urinary trypsin inhibitor (UTI, ulinastatin) was obtained from Mochida Pharmaceutical Co. (Shinjuku-ku, Tokyo, Japan) and used after dialysis against water. Bovine nasal cartilage proteoglycan (BNC–PG), chondroitinase ABC, chondroitinase AC-II, chondro-4-sulfatase, and standard samples of unsaturated disaccharides were obtained from Seikagaku Corp. (Chuo-ku, Tokyo, Japan). Calf intestine alkaline phosphatase was obtained from Roche Applied Science (Minato-ku, Tokyo, Japan). Aggrecan, decorin, and biglycan (all from bovine articular cartilage) were obtained from Sigma–Aldrich, Japan (Chuo-ku, Tokyo, Japan). 2-Aminobenzoic acid (2AA) and 2-aminoacridone (AMAC) were purchased from Tokyo Kasei Kogyo (Chuo-ku, Tokyo, Japan) and Molecular Probes (Eugene, OR, USA), respectively. DB-1 capillary, of which the inner surface is chemically modified with dimethylpolysiloxane, was obtained from J&W Scientific (Folsom, CA, USA). Polyethyleneglycol (PEG70000, average molecular mass 70,000) was from Wako Pure Chemicals (Dosho-machi, Osaka, Japan). Other reagents and solvents were of the highest grade commercially available.

Digestion of PGs with chondroitinase ABC

PG samples (100 μg) were dissolved in 50 mM Tris–HCl buffer (pH 8.0, 100 μl), and chondroitinase ABC (200 mU, 4 μl) dissolved in the same buffer was added to the solution. The enzyme reaction was carried out at 37 °C overnight, and the reaction mixture was passed through a filter device (M.W. 10,000 cutoff, Ultrafree-MC, Millipore) at 10,000*g* to separate the unsaturated disaccharides and core protein containing linkage oligosaccharides. After washing the core protein fraction with water (200 μl) by centrifugation three times, filtrate and washing (unsaturated disaccharides fraction) were combined and lyophilized to dryness by a centrifugal evaporator (SpeedVac, Servant). Lyophilized materials were used for fluorescent labeling with AMAC. The core protein containing linkage oligosaccharide in the filter cup was collected with water (100 μl) and used for releasing of oligosaccharides by AGC.

Release of oligosaccharides at the linkage region by AGC

To release oligosaccharides at the linkage region, the solution (100 μl) of core protein containing linkage oligosaccharides obtained by the method as described above was injected into AGC. An aqueous solution of 0.5 M LiOH was used as alkaline solution for releasing oligosaccharides at a flow rate of 0.5 ml/min, and temperature of the reaction coil in the reactor was set at 70 °C. After passing through the reactor, the reaction mixture was desalted by a cation-exchange cartridge in in-line mode. The eluate from the cation-exchange cartridge was collected into the sample reservoir by monitoring the absorbance at 230 nm. The process from sample injection to collection

of the released oligosaccharides was completed within 3 min. After the run, the cation-exchange cartridge was regenerated with 0.25 M H_2SO_4. The collected solution (ca. 900 μl) containing released oligosaccharides was lyophilized to dryness by a centrifugal evaporator, and the lyophilized material was used for fluorescent labeling with 2AA.

Fluorescent labeling of unsaturated disaccharides with AMAC

A mixture of unsaturated disaccharides obtained by the digestion with chondroitinase ABC was labeled with AMAC using the method reported previously [27]. Briefly, the mixture was dissolved in 100 mM AMAC in a mixture (10 μl) of dimethyl sulfoxide–acetic acid (17:3, v/v), and 1 M sodium cyanoborohydride (10 μl) in the same solvent was added. After maintaining the mixture at 90 °C for 30 min, water (500 μl) and chloroform (500 μl) were added to the reaction mixture and mixed vigorously by a vortex mixer. After removing the chloroform layer, the aqueous phase was washed again with chloroform (500 μl), and the procedure was repeated five times. A portion of the aqueous phase was used for the analysis by capillary electrophoresis (CE).

Fluorescent labeling of linkage oligosaccharides with 2AA

Released linkage oligosaccharides were derivatized with 2AA according to the method reported previously [28]. The linkage oligosaccharides released by AGC were dissolved in 2AA solution (100 μl) which was freshly prepared by dissolution of 2AA and sodium cyanoborohydride (15 mg each) in methanol (1 ml) containing 4% sodium acetate and 2% boric acid, and the mixture was kept at 80 °C for 1 h. After cooling, water (100 μl) was added to the mixture, and the mixture was applied on a column of Sephadex LH-20 (1 × 30 cm) previously equilibrated with 50% aqueous methanol. The earlier eluted fluorescent fractions were pooled and evaporated to dryness. The residue was dissolved in water (100 μl) and a portion of the solution was used for the analysis by capillary electrophoresis and MALDI-TOF MS.

Capillary electrophoresis

Capillary electrophoresis was performed on a Beckman MDQ Glycoprotein System. For the analysis of AMAC-labeled unsaturated disaccharides, electrophoresis was performed with a DB-1 capillary (50 μm i.d., 30 cm length) in 100 mM Tris–borate buffer (pH 8.0) containing 1% PEG70000, and detection was performed by an argon-laser-induced fluorescence detector (Ex 488 nm, Em 520 nm), whereas electrophoresis of 2AA-labeled linkage oligosaccharides was performed with a DB-1 capillary (100 μm i.d., 30 cm length) in 100 mM Tris–borate buffer (pH 8.0) containing 10% PEG, and detection was performed by a helium–cadmium–laser induced fluorescence detector (Ex 325 nm, Em 405 nm).

Chondro-4-sulfatase digestion

Digestion was performed according to the procedure recommended by the manufacturer. A portion of 2AA-labeled linkage oligosaccharides (7.6 nmol) was incubated with 20 mU of chondro-4-sulfatase in 50 mM Tris–HCl buffer (pH 7.5, 20 μl) containing 50 mM sodium acetate and 0.01% bovine serum albumin at 37 °C for 30 min. The reaction was terminated by maintaining the mixture on the boiling water bath for 5 min. A portion of the mixture (2 μl) was diluted with water (10 μl) and analyzed by capillary electrophoresis.

Chondroitinase AC-II digestion

Chondroitinase AC-II digestion was performed in a manner similar to that for chondro-4-sulfatase digestion. A portion of 2AA-labeled linkage oligosaccharides (7.6 nmol) was incubated with 25 mU of chondroitinase AC-II in 50 mM acetate buffer (pH 6.0) containing 50 mM sodium acetate and 0.01% bovine serum albumin at 37 °C for 30 min. After maintaining the mixture on the boiling water bath for 5 min, a portion of the mixture (2 μl) was diluted with water (10 μl) and analyzed by capillary electrophoresis.

MALDI-TOF MS

MALDI-TOF MS spectra of 2AA-labeled linkage oligosaccharides were acquired on a Voyager DE-Pro mass spectrometer (PE Biosystems, Framingham, MA, USA) in negative-ion linear mode. Nitrogen laser (337 nm) was used for the ionization. Accelerating voltage was 19 kV, and delayed extraction was performed after 500 ns. 2,5-Dihydroxybenzoic acid (DHB) was used as a matrix throughout the work.

Results

The outline of the method for the analysis of glycan portions of PGs is shown in Fig. 1. PGs afford a mixture of unsaturated disaccharides and the core protein bearing hexa- or higher oligosaccharides as linkage oligosaccharides by digestion with lyases [15]. In the present study, a sample of PG is extensively digested with chondroitinase ABC, and the reaction mixture is fractionated using a centrifugal filter device to two fractions of a mixture of unsaturated disaccharides and the protein portion to which linkage glycans are attached. The mixture of produced unsaturated disaccharides was labeled with AMAC and analyzed by CE. The protein core to which linkage oligosaccharides are attached is subjected to the automated glycan releasing apparatus, AutoGlycoCutter (AGC), to release oligosaccharides. The released oligosaccharides

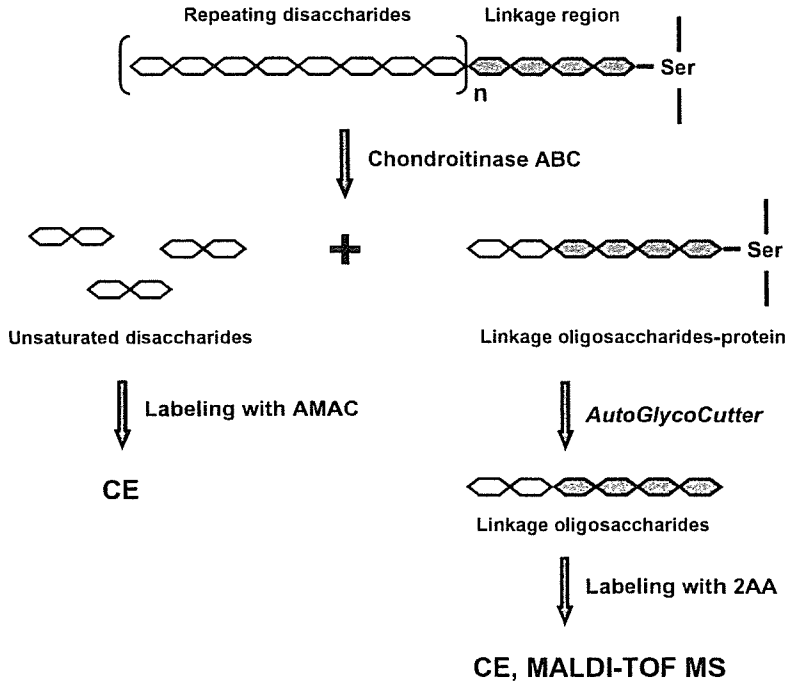

Fig. 1. Outline for the analysis of GAGs in PGs.

are then labeled with 2AA, and analyzed by CE and MALDI-TOF MS.

AGC is an apparatus for releasing *O*-linked-type oligosaccharides using an in-line flow system. AGC and the diagram of the system are shown in Fig. 2. AGC is an automated bench top apparatus composed of several units as shown in Fig. 2a. A portion (1–100 μl) of the sample solution of PGs after digestion with lyases as described above is introduced by an automatic injector into the flow of alkali solution supplied by a plunger pump at a flow rate of 0.1–1.5 ml/min. Glycans attached to the core protein through *O*-glycosidic linkages are released in the reaction coil (0.25 mm i.d., 10 m length) thermostated at constant temperature (40–150 °C) in the reactor. The alkaline solution containing released oligosaccharides is immediately cooled and neutralized by passing through a cartridge packed with cation-exchange resin (ca. 1 ml volume) to avoid further degradation of the released glycans. The effluent from the cartridge is detected by a UV absorption detector at 230 nm and the fractions containing released glycans are collected by a fraction collector. After the glycan-releasing reaction, the cartridge is regenerated with 0.25 M H_2SO_4 at a flow rate of 1.2 ml/min followed by washing with water by an automatic valve changing device.

Analysis of linkage oligosaccharides of UTI and efficiency in releasing reaction using AGC

Urinary trypsin inhibitor is a characteristic PG extracted from human urine [29,30] and used as a protease inhibitor for treatment of acute pancreatitis. UTI contains a low-sulfated chondroitin-4-sulfate chain at Ser10 [31,32] and has a disulfated hexasaccharide at the linkage region [33]. In the glycan-releasing reaction of UTI, we employed a reaction coil of 10 m length (0.25 mm i.d.) and 0.5 M LiOH as the alkali solution at a flow rate of 0.5 ml/min. Temperature of the reactor was set at 70 °C. Total time required for the releasing reaction of a PG sample was ca. 3 min. After the releasing reaction using AGC, we analyzed the linkage oligosaccharides as 2AA derivatives. The results were compared with those obtained by the conventional method reported previously (Fig. 3) [24]. In CE analysis, we employed a DB-1 capillary with the inner surface chemically modified with dimethylpolysiloxane. Therefore, oligosaccharides having higher negative charges move faster and are observed at earlier migration times. The linkage oligosaccharides released by AGC were observed nearly as a single peak at ca. 3 min (Fig. 3a). This result was clearly comparable with that obtained from the analysis of linkage oligosaccharides released by the conventional method (Fig. 3b). In MALDI-TOF MS analysis of 2AA-labeled linkage oligosaccharides obtained by the present method, a molecular ion at *m/z* 1311.9 corresponding to $[M+Na-2H]^-$ was observed (Fig. 3c) and, accordingly, the composition $\Delta HexAHexAHexNAcHex_2Pen(SO_3H)_2$ 2AA was predicted. A fragment ion at *m/z* 1209.9 due to loss of $NaSO_3^-$ ion was also observed. Similar results were also observed for the MALDI-TOF MS analysis of the oligosaccharides released by the conventional method (data not shown). MS analysis of polysulfated carbohydrates often gives fragment ions due to loss of sulfate groups [34]. After digestion with chondro-4-sulfatase, the major

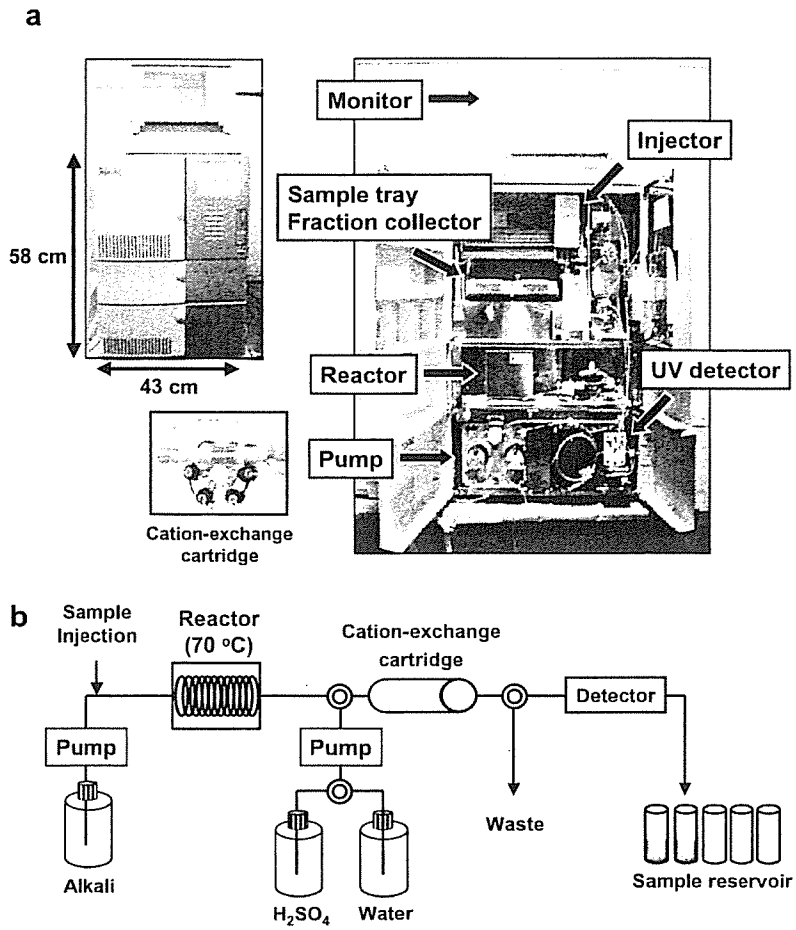

Fig. 2. AutoGlycoCutter (AGC) for releasing glycans from the core protein. (a) Appratus. (b) Diagram of AGC for oligosaccharide releasing.

peak at 3 min in CE was observed later at ca. 4.4 min as a single peak (data not shown). Chondro-4-sulfatase has been demonstrated to release the sulfate groups at C4 position of Gal and that of GalNAc in the disulfated hexasaccharide [10]. From these results, we concluded that AGC gave results similar to those obtained by the conventional method, and the oligosaccharide released by AGC has the following structure as reported previously [33]: ΔHexAα1-3GalNAc(4-sulfate)β1-4GlcAβ1-3Gal(4-sulfate)-β1-3Galβ1-4Xyl-2AA. Efficiency in recovery of oligosaccharides at the linkage region was $64 \pm 3\%$ ($n = 7$) as determined by CE.

Evaluation of AGC using model PGs

PG derived from bovine nasal cartilage is a high-molecular-weight PG that contains up to 150 chondroitin sulfate chains and 30–50 keratan sulfate chains [11,35]. The GAG chains are attached to the core protein through *O*-glycosidic linkages. The hexasaccharides derived from the linkage region have both C4 and C6 sulfate groups [11]. In a manner similar to that described above, we analyzed the oligosaccharides derived from the linkage region of BNC–PG by CE after the releasing reaction followed by derivatization with 2AA (Fig. 4). Peaks **2** and **3** were assigned as monosulfated hexasaccharides, and peak **4** was assigned as nonsulfated hexasaccharides from their migration times. Upon digestion of the mixture of linkage oligosaccharides of BNC–PG with chondro-4-sulfatase, the peaks observed at 2.9 and 3.4 min (peaks **1** and **2**) disappeared and the relative intensity of peak **4** increased. We also found that peaks **2** and **3** were shifted to later migration times after digestion with chondroitinase AC-II (data not shown). These results indicate that a sulfate group in the hexasaccharides observed as peaks **2** and **3** is on the GalNAc residue. The results are also confirmed by MS data as shown in Fig. 4c. The linkage oligosaccharides derived from BNC–PG showed two ions at *m/z* 1210.9 and *m/z* 1130.8 which correspond to monosulfated hexasaccharides (ΔHexA-HexAHexNAcHex$_2$Pen(SO_3H)2AA) and nonsulfated hexasaccharides (ΔHexAHexAHexNAcHex$_2$Pen2AA), respectively. From these observations, it was revealed that peak **1** is a disulfated hexasaccharide as a minor component, and peak **2** is a hexasaccharide that has a sulfate group at the C4 position of the GalNAc residue. In a previous study, it was demonstrated that the monosulfated

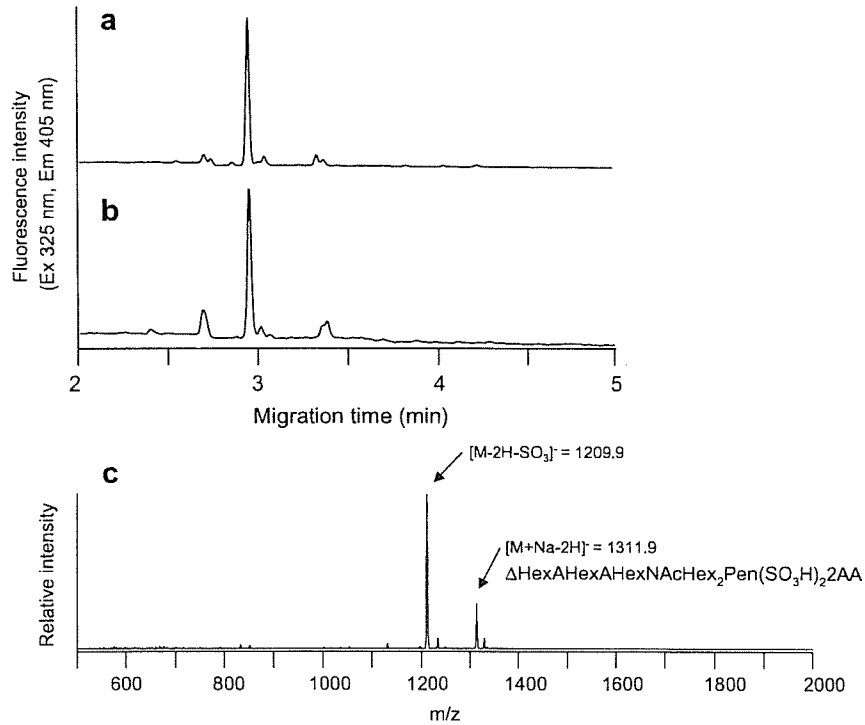

Fig. 3. CE and MALDI-TOF MS analysis of 2AA-labeled linkage oligosaccharides derived from UTI. 2AA-labeled oligosaccharides released by AGC (a) and the conventional in-tube method (b) were analyzed by CE. Analytical conditions for CE; capillary, DB-1 capillary (30 cm × 100 μm i.d.); running buffer, 100 mM Tris–borate buffer (pH 8.0) containing 10% PEG70000; applied voltage, 20 kV; injection, pressure method (1.0 psi for 10 s); temperature, 25 °C; detection, helium–cadmium laser-induced fluorescence (Ex: 325 nm, Em: 405 nm). (c) MALDI-TOF MS spectra of 2AA-labeled linkage oligosaccharides.

hexasaccharides derived from the linkage region of bovine nasal septal cartilage PG were sulfated at either the C4 or the C6 position of the GalNAc residue [11]. Accordingly, we concluded that peak **3**, which was resistant to chondro-4-sulfatase, is hexasaccharide sulfated at the C6 position of the GalNAc residue. Structures of the linkage hexasaccharides observed in BNC–PG are summarized and relative abundances of glycans estimated from their peak areas in CE analysis are shown in Table 1. The relative abundances of glycans observed in BNC–PG were slightly different from those reported previously [11]. The reasons for this difference may be due to the difference of PG material used because de Beer et al. [11] used a more limited part of nasal cartilage (septal) as a source of PG, while KS chains in BNC–PG were not observed in the present study and further studies are required.

Aggrecan is the major proteoglycan in articular cartilage and is important for proper functioning of articular cartilage. Aggrecan derived from bovine articular cartilage has chondroitin-6-sulfate chains as major GAGs, and their linkage-region oligosaccharides were sulfated at the C6 position predominantly [15,16]. We released the oligosaccharides at the linkage region of aggrecan by AGC and analyzed them after labeling with 2AA (Fig. 5). Two major peaks were observed at 3.4 and 4.1 min (Fig. 5a). The glycan (peak **1**) has one sulfate group in the molecule. These peaks were not digested with chondro-4-sulfatase and calf intestine alkaline phosphatase (data not shown). Thus, we concluded that peaks **1** and **2** are hexasaccharides having a sulfate group at the C6 position of the GalNAc residue and nonsulfated hexasaccharide, respectively. This result was also supported by MALDI-TOF MS analysis (Fig. 5b). The oligosaccharides derived from the linkage region of aggrecan showed an abundant ion at *m/z* 1209.6 of monosulfated hexasacchride (ΔHexAHexAHexNAcHex$_2$Pen(SO$_3$H)2AA) with its sodium adduct ion (*m/z* 1232) and a small ion peak at *m/z* 1129.3 of nonsulfated hexasaccharide (ΔHexAHexAHexNAcHex$_2$Pen2AA). The structures and relative abundances of these hexasaccharides are also summarized in Table 1. Relative abundances of hexasaccharides at the linkage region observed in aggrecan also showed values slightly different from those reported previously [16].

Decorin, which is a member of the small leucine-rich PG family, plays a key role as a modulator of cell growth by interaction with matrix components or a variety of other proteins such as fibronectin or transforming growth factor-β [36]. Recently, decorin was reported to increase in human colon adenocarcinomas with significant structure changes [6]. Mammalian decorin has a single CS/DS chain that is attached to Ser4 [37]. We analyzed the oligosaccharides at the linkage region of the CS/DS chain of decorin

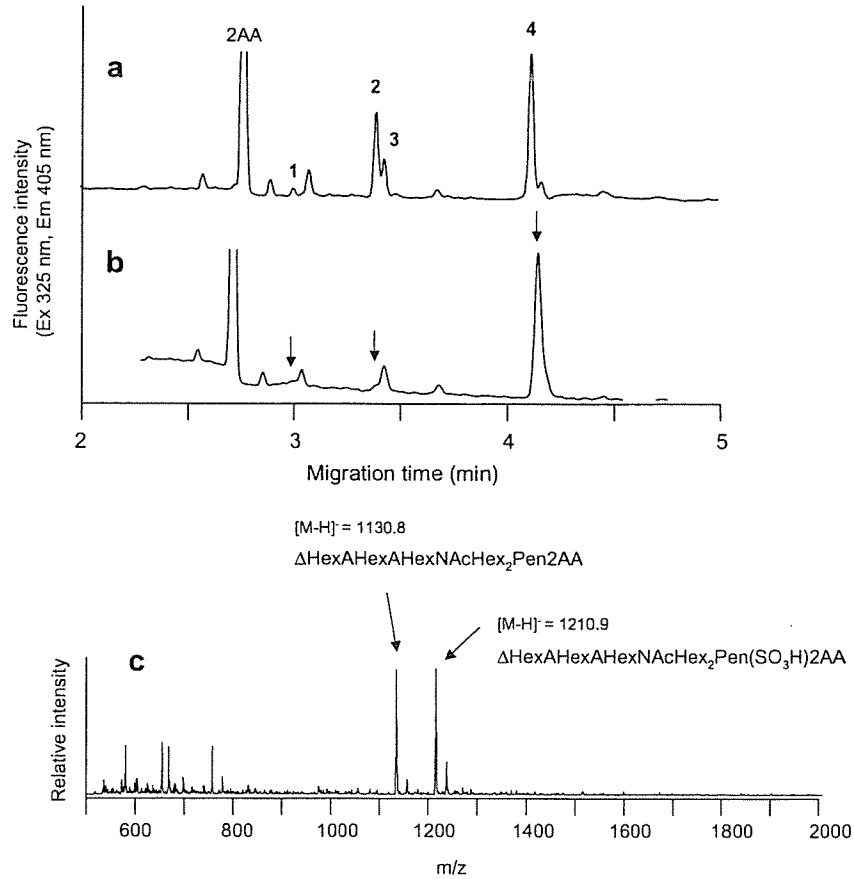

Fig. 4. CE and MALDI-TOF MS analysis of 2AA-labeled linkage oligosaccharides derived from BNC–PG. 2AA-labeled linkage oligosaccharides derived from BNC–PG were analyzed by CE before digestion (a) and after digestion with chondro-4-sulfatase (b). Analytical conditions for CE were the same as those described in Fig. 3. Arrows indicate the peaks changed after digestion. (c) MALDI-TOF MS spectra of 2AA-labeled linkage oligosaccharides.

derived from bovine articular cartilage. The results of CE and MALDI-TOF MS analysis are shown in Fig. 6. In CE analysis of the 2AA-labeled oligosaccharides, monosulfated hexasaccharides (peaks **2** and **3**) and nonsulfated hexasaccharide (peak **4**) were observed at 3.3 and 4.3 min, respectively, as major components (Fig. 6a). A broad peak (peak **1**) due to disulfated hexasaccharides was also observed at ca. 2.7 min as minor components. After digestion with chondro-4-sulfatase, peak **2** was shifted to the position of peak **4** (Fig. 6b) but peak **3** was not digested with alkaline phosphatase (data not shown). These results clearly indicated that peaks **2** and **3** were the C4 and C6 sulfated hexasaccharide, respectively. After digestion with chondroitinase AC-II, the 2AA-labeled linkage oligosaccharides gave two peaks at 3.3 and 4.3 min, respectively (Fig. 6c). The major peak observed at 4.3 min seems to be the linkage tetrasaccharide ΔHexAβ1-3Galβ1-3Galβ1-4Xyl-2AA from its migration time. A portion of the minor peak observed at 3.3 min, which is resistant to chondroitinase AC-II, is probably due to iduronic acid-containing hexasaccharide because chondroitinase AC-II does not act on this hexasaccharide [38]. This type of oligosaccharide which contains iduronic acid was also found in recombinant decorin expressed in Chinese hamster ovary cells [39]. MALDI-TOF MS analysis showed a molecular ion at *m/z* 1210.9 corresponding to monosulfated hexasaccharides ($\Delta HexAHexAHexNAcHex_2Pen(SO_3H)2AA$) and a minor ion at *m/z* 1130.9 due to nonsulfated hexasaccharide ($\Delta HexAHexAHexNAcHex_2Pen2AA$) (Fig. 6d). The results are summarized in Table 1. The broad peak (peak **1**) of disulfated hexasaccharides indicates that the sulfation patterns of disulfated hexasaccharides are highly heterogenous.

Biglycan is also a member of the small leucine-rich PG family and usually has two CS/DS chains attached to Ser5 and Ser11 [40]. We analyzed the oligosaccharides at the linkage region of CS/DS chains of biglycan derived from bovine articular cartilage and compared them with those of decorin. The results are shown in Fig. 7. In CE analysis, the oligosaccharides derived from biglycan showed an electropherogram similar to that observed for the analysis of oligosaccharides derived from decorin (Fig. 7a), but the oligosaccharide composition was different from that of decorin. After digestion with chondro-4-sulfatase, peak **2** disappeared and peak **4** increased (Fig. 7b) but peak **3** was not digested with alkaline phosphatase (data

Table 1
Structures and relative abundances of linkage oligosaccharides derived from PGs

Peak No.[a]	Structure[b]	Relative abundance (%)[c]
BNC–PG		
1	ΔHexAα1-3GalNAc(4S)β1-4GlcAβ1-3Gal(4S)β1-3Galβ1-4Xyl-2AA	2 (11)
2	ΔHexAα1-3GalNAc(4S)β1-4GlcAβ1-3Galβ1-3Galβ1-4Xyl-2AA	28 (43)
3	ΔHexAα1-3GalNAc(6S)β1-4GlcAβ1-3Galβ1-3Galβ1-4Xyl-2AA	14 (6)
4	ΔHexAα1-3GalNAcβ1-4GlcAβ1-3Galβ1-3Galβ1-4Xyl-2AA	56 (38)
Aggrecan		
1	ΔHexAα1-3GalNAc(6S)β1-4GlcAβ1-3Galβ1-3Galβ1-4Xyl-2AA	56 (68)
2	ΔHexAα1-3GalNAcβ1-4GlcAβ1-3Galβ1-3Galβ1-4Xyl-2AA	44 (32)
Decorin		
1	ΔHexAα1-3GalNAc(S)β1-4GlcAβ1-3Gal(S)β1-3Galβ1-4Xyl-2AA	21
2	ΔHexAα1-3GalNAc(4S)β1-4GlcAβ1-3Galβ1-3Galβ1-4Xyl-2AA	5
2	ΔHexAα1-3GalNAc(4S)β1-4IdoAα1-3Galβ1-3Galβ1-4Xyl-2AA	16
3	ΔHexAα1-3GalNAc(6S)β1-4GlcAβ1-3Galβ1-3Galβ1-4Xyl-2AA	41
4	ΔHexAα1-3GalNAcβ1-4GlcAβ1-3Galβ1-3Galβ1-4Xyl-2AA	17
Biglycan		
1	ΔHexAα1-3GalNAc(S)β1-4GlcAβ1-3Gal(S)β1-3Galβ1-4Xyl-2AA	10
2	ΔHexAα1-3GalNAc(4S)β1-4GlcAβ1-3Galβ1-3Galβ1-4Xyl-2AA	15
2	ΔHexAα1-3GalNAc(4S)β1-4IdoAα1-3Galβ1-3Galβ1-4Xyl-2AA	1
3	ΔHexAα1-3GalNAc(6S)β1-4GlcAβ1-3Galβ1-3Galβ1-4Xyl-2AA	45
4	ΔHexAα1-3GalNAcβ1-4GlcAβ1-3Galβ1-3Galβ1-4Xyl-2AA	29

[a] Peaks observed in CE analysis.
[b] Previously reported oligosaccharide structure.
[c] Values in parentheses are previously reported.

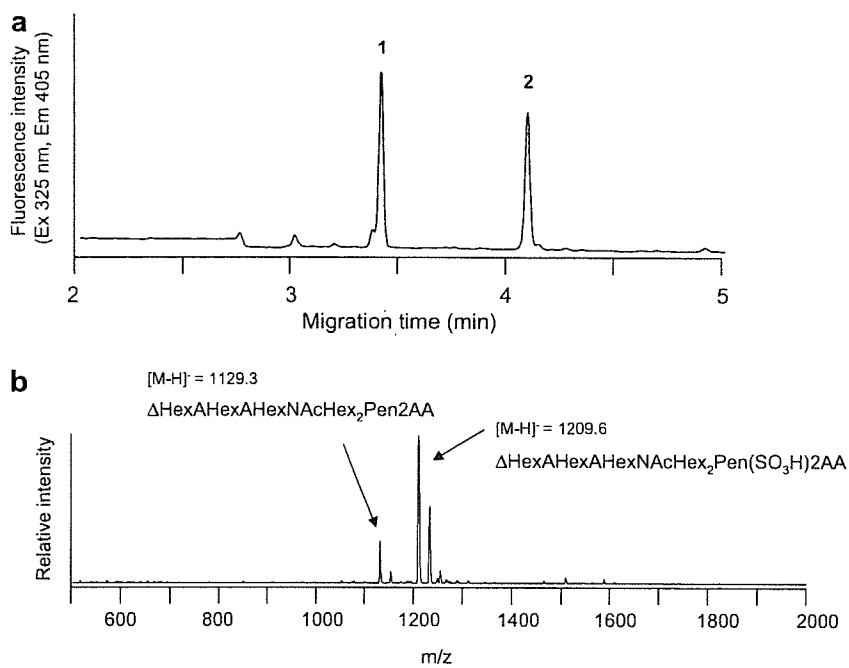

Fig. 5. CE and MALDI-TOF MS analysis of 2AA-labeled linkage oligosaccharides derived from aggrecan. 2AA-labeled linkage oligosaccharides derived from aggrecan were analyzed by CE (a) and MALDI-TOF MS (b). Analytical conditions for CE were the same as those described in Fig. 3.

not shown). After digestion with chondroitinase AC-II, the 2AA-labeled linkage oligosaccharides in biglycan gave a peak at 4.3 min and a small peak of iduronic acid-containing hexasaccharide at 3.3 min (Fig. 7c). In MALDI-TOF MS analysis, the 2AA-labeled linkage oligosaccharides derived from biglycan showed two major molecular ions at *m/z* 1210.3 and *m/z* 1130.1 due to monosulfated hexasaccharides (ΔHexAHexAHexNAcHex$_2$Pen(SO$_3$H)2AA) and nonsulfated hexasaccharide (ΔHexAHexAHexNAcHex$_2$Pen2AA), respectively (Fig. 7d). The list of linkage

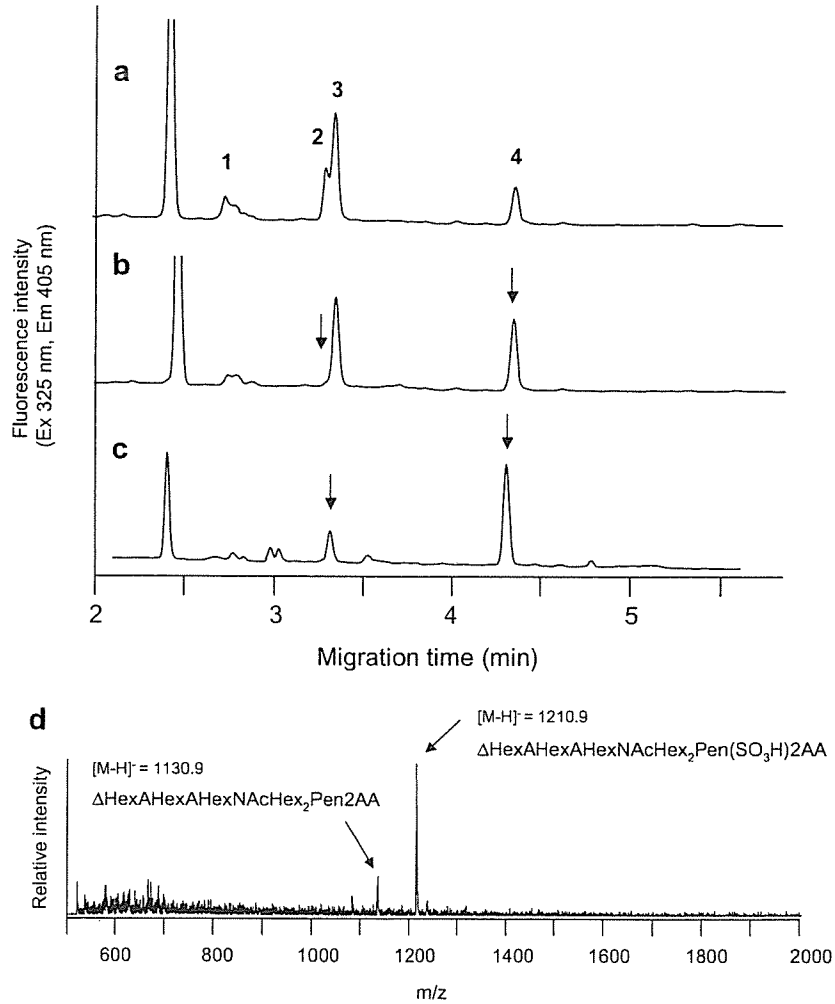

Fig. 6. CE and MALDI-TOF MS analysis of 2AA-labeled linkage oligosaccharides derived from decorin. 2AA-labeled linkage oligosaccharides derived from decorin were analyzed by CE before digestion (a) and after digestion with chondro-4-sulfatase (b) and chondroitinase AC-II (c). Analytical conditions for CE were the same as those described in Fig. 3. Arrows indicate the peaks changed after digestion. (d) MALDI-TOF MS spectra of 2AA-labeled linkage oligosaccharides.

oligosaccharides observed in biglycan is summarized in Table 1.

Disaccharide composition analysis

Disaccharide units of CS chains in PG samples employed in the present study were determined. The mixture of unsaturated disaccharides obtained by digestion with chondroitinase ABC was labeled with AMAC and analyzed by CE according to the procedure described in Fig. 1. The results are shown in Fig. 8. UTI gave two major peaks of Δdi-4S and Δdi-0S at 3.4 and 5.3 min, respectively (Fig. 8a). BNC–PG showed a nearly single peak of Δdi-4S at 3.4 min (Fig. 8b), while aggrecan, decorin and biglycan gave Δdi-6S at 3.3 min and the peak of Δdi-4S (Figs. 8c–e) as the major disaccharides. The disaccharide compositions estimated by peak areas are summarized in Table 2. The relative ratios of disaccharides derived from UTI were 37.2% for Δdi-4S and 62.8% for Δdi-0S. BNC–PG showed a high proportion of Δdi-4S (90.7%), and contained Δdi-6S (9.3%) and a trace amount of Δdi-0S. The major disaccharides derived from aggrecan were Δdi-6S (70.2%), Δdi-4S (21.1%), and Δdi-0S (8.7%). Decorin and biglycan showed both Δdi-4S and Δdi-6S as major components, but biglycan showed higher Δdi-6S content than that observed in decorin. The relative ratios of disaccharides derived from UTI, BNC–PG, and aggrecan showed good agreement with the reported data [11,15,32], but those of disaccharides derived from decorin and biglycan were slightly different [41].

Discussion

We proposed a method for the rapid analysis of oligosaccharides at the GAGs–protein linkage region. To shorten the total time required for the analysis of linkage oligosaccharides in PGs, we fabricated an automatic

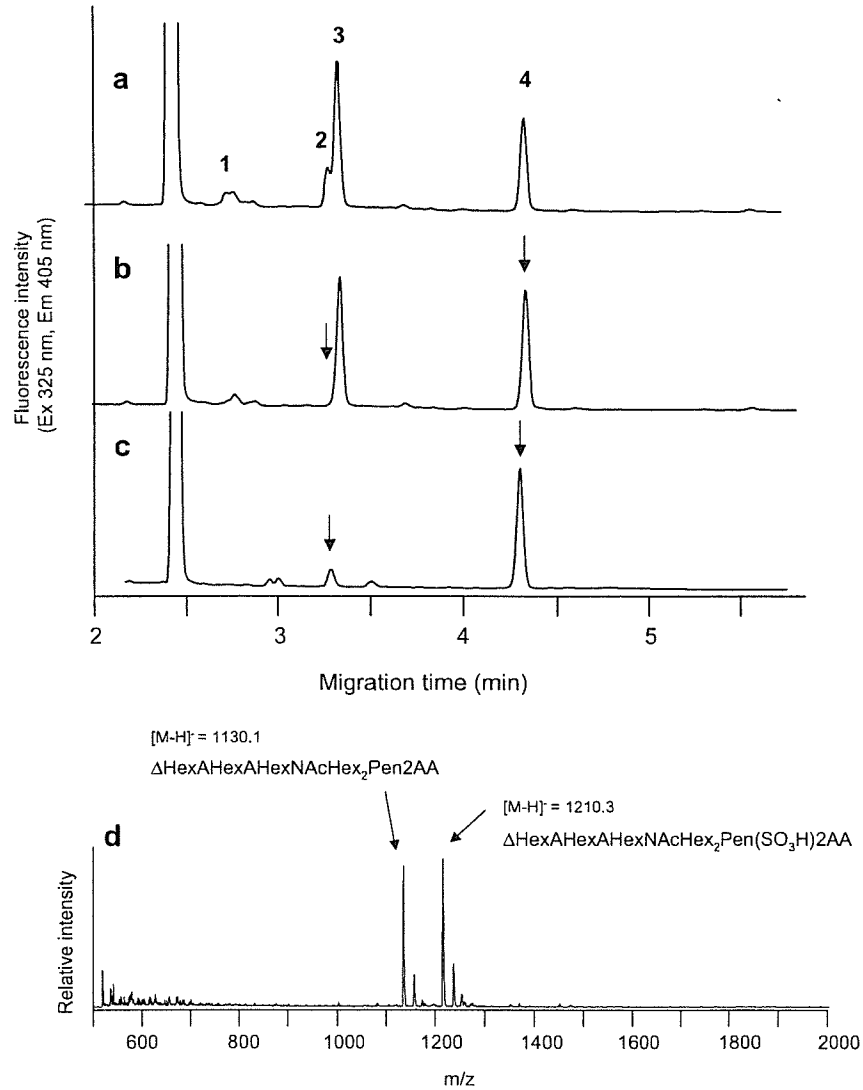

Fig. 7. CE and MALDI-TOF MS analysis of 2AA-labeled linkage oligosaccharides derived from biglycan. 2AA-labeled linkage oligosaccharides derived from biglycan were analyzed by CE (a). (b) and (c) are the results after digestion with chondro-4-sulfatase and chondroitinase AC-II, respectively. Analytical conditions for CE were the same as those described in Fig. 3. Arrows indicate the peaks changed after digestion. (d) MALDI-TOF MS spectra of 2AA-labeled linkage oligosaccharides.

carbohydrate releasing apparatus (AutoGlycoCutter) for rapid release of linkage oligosaccharides by employing the in-line flow system. By using AGC, the time required for release of oligosaccharides is only ca. 3 min, and we can achieve ca. 1000-fold rapid release of oligosaccharides compared to that required by the conventional in-tube method. In addition, it should be noted that analyses of 2AA-labeled oligosaccharides at the linkage region and AMAC-labeled unsaturated disaccharides by CE were completed within 5 and 10 min, respectively. Although the analysis of oligosaccharides at the linkage region has so far been generally performed by HPLC, we demonstrated that CE will be a useful technique. Furthermore, in MALDI-TOF MS analysis, sulfate groups can be lost through fragmentation. Therefore, to analyze the sulfated glycans such as linkage oligosaccharides, it is essential to employ chromatographic techniques such as CE in addition to MALDI-TOF MS. The efficiency of the releasing reaction by the present method was lower than that by the conventional method and was different among the PGs used (57–73% relative to those by the conventional method). However, the profiles obtained by the present method showed separation profiles quite similar to those obtained by the conventional in-tube method. Furthermore, it should be noted that the in-line flow system, in principle, shows excellent reproducibility.

The results of the analysis of linkage oligosaccharide in UTI by a combination of CE and MALDI-TOF MS revealed that AGC could release the linkage oligosaccharides from the protein core without any loss of sulfate groups or degradation of carbohydrate chains due to peeling reaction. We also analyzed the linkage oligosaccharides

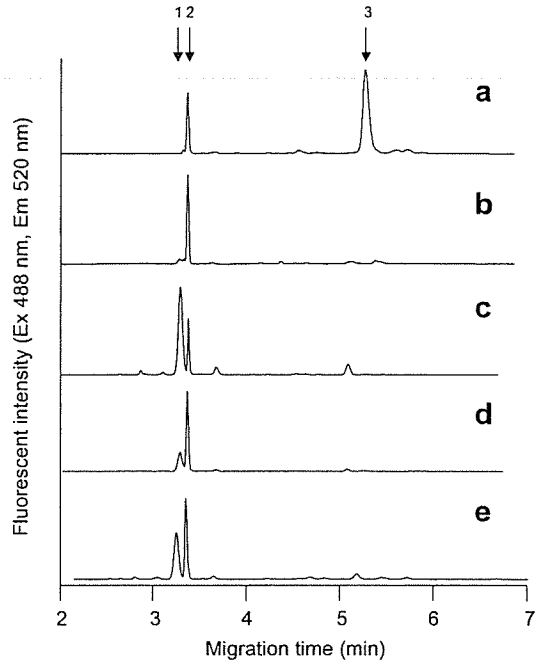

Fig. 8. Disaccharides composition analysis of PGs. AMAC-labeled unsaturated disaccharides derived from (a) UTI, (b) BNC–PG, (c) aggrecan, (d) decorin, and (e) biglycan were analyzed by CE. Analytical conditions for CE; capillary, DB-1 capillary (30 cm × 50 μm i.d.); running buffer, 100 mM Tris–borate buffer (pH 8.0) containing 1% PEG70000; applied voltage, 20 kV; injection, pressure method (1.0 psi for 10 s); temperature, 25 °C; detection, argon-laser-induced fluorescence (Ex: 488 nm, Em: 520 nm). Arrows indicate the migration position of the authentic unsaturated chondro-disaccharides: 1, Δdi-6S; 2, Δdi-4S; 3, Δdi-0S.

Table 2
Disaccharides compositions of PGs

PGs	Disacchride (%)		
	Δdi-6S	Δdi-4S	Δdi-0S
UTI	0	37.2	62.8
BNC–PG	9.3	90.7	Trace
Aggrecan	70.2	21.1	8.7
Decorin	30.4	65.0	3.7
Biglycan	48.9	45.3	5.8

derived from five commercially available CS/DS–PGs to evaluate the performance of AGC.

Because the sulfated Gal structures have not been found in the linkage region of HP/HS–PGs, sulfate groups at the Gal residues are considered to be biological signals for CS/DS biosynthesis. It has been reported that CS chains of BNC–PG contain Δdi-4S unit predominantly [11,35]. Similar results were observed in disaccharide composition analysis (Table 2). In contrast, aggrecan gave more complex mixtures of disaccharides composed of Δdi-6S and Δdi-4S units as major components and small amounts of Δdi-0S unit (Table 2). However, in contrast to the results observed in disaccharides composition analysis, monosulfated hexasaccharides of BNC–PG at the linkage region were those sulfated at both the C4 and the C6 positions of the GalNAc residues (the molar ratio of C4 sulfated and C6 sulfated is ca. 2:1), but the GalNAc residues of aggrecan were sulfated only at the C6 position (Table 1). These results indicated that sulfation patterns observed in the linkage region are markedly different from those observed in the disaccharides repeating region.

It should be noted that BNC–PG and aggrecan also contain keratan sulfate chains mostly attached through *O*-linked glycosides [42]. The core structure of KS is not the PG type but is the mucin type. The nonreducing glycan portions were not eliminated by the digestion with chondroitinases. Accordingly, the released oligosaccharides were not observed by the present method, and further studies may be required for the analysis of KS. In the present study, phosphorylated Xyl structure was not confirmed because the linkage oligosaccharides in CS/DS–PGs used in the present study do not contain this structure [11,15,16,39]. Accordingly, the stability of phosphoesters under the present conditions must be tested in the future.

The results obtained from comparison of the linkage oligosaccharides of decorin with those of biglycan demonstrated that the content of iduronic acid-containing hexasaccharides of biglycan was significantly lower than that of decorin (Table 1). The iduronic acid-containing linkage oligosaccharide is a DS-specific structure [38]. DS is a copolymer of two types of disaccharide unit, which are D-glucuronic acid and L-iduronic acid containing units, and the content of the iduronic acid-containing unit and the sulfation patterns of DS are highly tissue specific. It has been reported that CS/DS chains of decorin and biglycan derived from bovine articular cartilage bear exclusively C4 sulfation [41]. Our results indicate that decorin and biglycan showed high proportions of Δdi-6S, especially biglycan, which are different from the results in the previous report. However, biglycan exhibited a small proportion of the iduronic acid-containing linkage-region oligosaccharide. This observation may correlate with the results of the high proportion of the Δdi-6S.

In the present study, we could not show applications for heparin/heparan sulfate-type PGs because it is difficult to obtain standard samples of heparin/heparan sulfate-type PGs. However, the present method will be applicable to the analysis of heparin/heparan sulfate-type PGs by using a combination of specific enzymes such as heparinase and heparitinase.

In conclusion, the present procedure for the analysis of the glycan part of PGs allows rapid and sensitive analysis of GAGs, will be a powerful tool for routine analysis of PGs, and provides an easy and rapid tool for studying biosynthesis of GAGs.

Acknowledgment

This work was supported by the New Energy and Industrial Technology Development Organization.

References

[1] N.B. Schwartz, Biosynthesis and regulation of expression of proteoglycans, Front. Biosci. 5 (2000) 649–655.

[2] L.Å. Fransson, Structure and function of cell-associated proteoglycans, Trends Biochem. Sci. 12 (1987) 406–411.

[3] L. Ameye, M.F. Young, Mice deficient in small leucine-rich proteoglycans: novel in vivo models for osteoporosis, osteoarthritis, Ehlers-Danlos syndrome, muscular dystrophy, and corneal diseases, Glycobiology 12 (2002) 107R–116R.

[4] E. Forsberg, L. Kjellen, Heparan sulfate: lessons from knockout mice, J. Clin. Invest. 108 (2001) 175–180.

[5] R.V. Iozzo, Matrix proteoglycans: from molecular design to cellular function, Annu. Rev. Biochem. 67 (1998) 609–652.

[6] A.D. Theocharis, Human colon adenocarcinoma is associated with specific post-translational modifications of versican and decorin, Biochim. Biophys. Acta 1588 (2002) 165–172.

[7] R.V. Iozzo, The biology of the small leucine-rich proteoglycans. Functional network of interactive proteins, J. Biol. Chem. 274 (1999) 18843–18846.

[8] K. Sugahara, I. Yamashina, P. de Waard, H. van Halbeek, J.F.G. Vliegenthart, Structural studies on sulfated oligosaccharides from carbohydrate–protein linkage region of chondroitin 4-sulfate proteoglycans of swarm rat chondrosarcoma, J. Biol. Chem. 263 (1988) 10168–10174.

[9] K. Sugahara, H. Kitagawa, Recent advances in the study of the biosynthesis and functions of sulfated glycosaminoglycans, Curr. Opin. Struct. Biol. 10 (2000) 518–527.

[10] K. Sugahara, M. Masuda, T. Harada, I. Yamashina, P. de Waard, J.F.G. Vliegenthart, Structural studies on sulfated oligosaccharides derived from the carbohydrate–protein linkage region of chondroitin sulfate proteoglycans of whale cartilage, Eur. J. Biochem. 202 (1991) 805–811.

[11] T. de Beer, A. Inui, H. Tsuda, K. Sugahara, J.F.G. Vliegenthart, Polydispersity in sulfation profile of oligosaccharide alditols isolated from the protein-linkage region and the repeating disaccharide region of chondroitin 4-sulfate of bovine nasal septal cartilage, Eur. J. Biochem. 240 (1996) 789–797.

[12] F. Cheng, D. Heinegård, L.Å. Fransson, M. Bayliss, J. Bielicki, J. Hopwood, K. Yoshida, Variations in the chondroitin sulfate–protein linkage region of aggrecans from bovine nasal and human articular cartilages, J. Biol. Chem. 271 (1996) 28572–28580.

[13] P. de Waard, J.F.G. Vliegenthart, T. Harada, K. Sugahara, Structural studies on sulfated oligosaccharides derived from the carbohydrate–protein linkage region of chondroitin 6-sulfate proteoglycans of shark cartilage. II. 7 compounds containing 2 or 3 sulfate residues, J. Biol. Chem. 267 (1992) 6036–6043.

[14] K. Sugahara, Y. Ohi, T. Harada, P. de Waard, J.F.G. Vliegenthart, Structural studies on sulfated oligosaccharides derived from the carbohydrate–protein linkage region of chondroitin 6-sulfate proteoglycans of shark cartilage. I. Six compounds containing 0 or 1 sulfate and/or phosphate residues, J. Biol. Chem. 267 (1992) 6027–6035.

[15] R.M. Lauder, T.N. Huckerby, I.A. Nieduszynski, Increased incidence of unsulphated and 4-sulphated residues in the chondroitin sulphate linkage region observed by high-pH anion-exchange chromatography, Biochem. J. 347 (2000) 339–348.

[16] T.N. Huckerby, R.M. Lauder, I.A. Nieduszynski, Structure determination for octasaccharides derived from the carbohydrate–protein linkage region of chondroitin sulphate chains in the proteoglycan aggrecan from bovine articular cartilage, Eur. J. Biochem. 258 (1998) 669–676.

[17] K. Sugahara, S. Yamada, K. Yoshida, P. de Waard, J.F.G. Vliegenthart, A novel sulfated structure in the carbohydrate–protein linkage region isolated from porcine intestinal heparin, J. Biol. Chem. 267 (1992) 1528–1533.

[18] K. Sugahara, R. Tohno-oka, S. Yamada, K.H. Khoo, H.R. Morris, A. Dell, Structural studies on the oligosaccharides isolated from bovine kidney heparan sulphate and characterization of bacterial heparitinase used as substrates, Glycobiology 4 (1994) 535–544.

[19] L.Å. Fransson, I. Silverberg, I. Carlstedt, Structure of the heparan sulfate–protein linkage region. Demonstration of the sequence galactosyl-galactosyl-xylose-2-phosphate, J. Biol. Chem. 260 (1985) 14722–14726.

[20] M. Ueno, S. Yamada, M. Zako, M. Bernfield, K. Sugahara, Structural characterization of heparan sulfate and chondroitin sulfate of Syndecan-1 purified from normal murine mammary gland epithelial cells. Common phosphorylation of xylose and differential sulfation of galactose in the protein linkage region tetrasaccharide sequence, J. Biol. Chem. 276 (2001) 29134–29140.

[21] J. Moses, Å. Oldberg, F. Cheng, L.Å. Fransson, Biosynthesis of the proteoglycan decorin—transient 2-phosphorylation of xylose during formation of the trisaccharide linkage region, Eur. J. Biochem. 248 (1997) 521–526.

[22] J. Moses, Å. Oldberg, L.Å. Fransson, Initiation of galactosaminoglycan biosynthesis. Separate galactosylation and dephosphorylation pathways for phosphoxylosylated decorin protein and exogenous xyloside, Eur. J. Biochem. 260 (1999) 879–884.

[23] L.C. Pedersen, K. Tsuchida, H. Kitagawa, K. Sugahara, T.A. Darden, M. Negishi, Heparan/chondroitin sulfate biosynthesis. Structure and mechanism of human glucuronyltransferase I, J. Biol. Chem. 275 (2000) 34580–34585.

[24] H. Sakaguchi, M. Watanabe, C. Ueoka, E. Sugiyama, T. Taketomi, S. Yamada, K. Sugahara, Isolation of reducing oligosaccharide chains from the chondroitin/dermatan sulfate-protein linkage region and preparation of analytical probes by fluorescent labeling with 2-aminobenzamide, J. Biochem. 129 (2001) 107–118.

[25] K. Takagaki, A. Kon, H. Kawasaki, T. Nakamura, S. Tamura, M. Endo, Isolation and characterization of Patnopecten mid-gut gland endo-beta-xylosidase active on peptidochondroitin sulfate, J. Biol. Chem. 265 (1990) 854–860.

[26] K. Takagaki, M. Iwafune, I. Kakizaki, K. Ishido, Y. Kato, M. Endo, Cleavage of the xylosyl serine linkage between a core peptide and a glycosaminoglycan chain by cellulases, J. Biol. Chem. 277 (2002) 18397–18403.

[27] Y. Matsuno, M. Kinoshita, K. Kakehi, Electrophoretic analysis of di- and oligosaccharides derived from glycosaminoglycans on microchip format, J. Pharm. Biomed. Anal. 36 (2004) 9–15.

[28] M. Nakano, K. Kakehi, M.H. Tsai, Y.C. Lee, Detailed structural features of glycan chains derived from alpha1-acid glycoproteins of several different animals: The presence of hypersialylated, O-acetylated sialic acids but not disialyl residues, Glycobiology 14 (2004) 431–441.

[29] B.J. Bromke, F. Kueppers, The major urinary protease inhibitor: simplified purification and characterization, Biochem. Med. 27 (1982) 56–67.

[30] Y. Tanaka, S. Maehara, H. Sumi, N. Toki, S. Moriyama, K. Sasaki, Purification and partial characterization of two forms of urinary trypsin inhibitor, Biochim. Biophys. Acta 705 (1982) 192–199.

[31] K. Hochstrasser, O.L. Schonberger, I. Rossmanith, E. Wachter, Kunitz-type proteinase inhibitors derived by limited proteolysis of the inter-alpha-trypsin inhibitor, V. Attachments of carbohydrates in the human urinary trypsin inhibitor isolated by affinity chromatography, Hoppe-Seyler's Z. Physiol. Chem. 362 (1981) 1357–1362.

[32] H. Toyoda, S. Kobayashi, S. Sakamoto, T. Toida, T. Imanari, Structural analysis of a low-sulfated chondroitin sulfate chain in human urinary trypsin inhibitor, Biol. Pharm. Bull. 16 (1993) 945–947.

[33] S. Yamada, M. Oyama, Y. Yuki, K. Kato, K. Sugahara, The uniform galactose 4-sulfate structure in the carbohydrate-protein linkage region of human urinary trypsin inhibitor, Eur. J. Biochem. 233 (1995) 687–693.

[34] N.S. Gunay, K. Tadano-Aritomi, T. Toida, I. Ishizuka, R.J. Linhardt, Evaluation of counterions for electrospray ionization mass spectral analysis of a highly sulfated carbohydrate, sucrose octasulfate, Anal. Chem. 75 (2003) 3226–3231.

[35] P. Flodin, J.D. Gregory, L. Rodén, Separation of acidic oligosaccharides by gel filtration, Anal. Biochem. 8 (1964) 424–433.
[36] R.V. Iozzo, A.D. Murdoch, Proteoglycans of the extracellular environment: clues from the gene and protein side offer novel perspectives in molecular diversity and function, FASEB J. 10 (1996) 598–614.
[37] R.K. Chopra, C.H. Pearson, G.A. Pringle, D.S. Fackre, P.G. Scott, Dermatan sulfate is located on serine-4 of bovine skin proteodermatan sulphate. Demonstration that most molecules possess only one glycosaminoglycan chain and comparison of amino acid sequences around glycosylation sites in different proteoglycans, Biochem. J. 232 (1985) 277–279.
[38] K. Sugahara, Y. Ohkita, Y. Shibata, K. Yoshida, A. Ikegami, Structural studies on the hexasaccharide alditols isolated from the carbohydrate–protein linkage region of dermatan sulfate proteoglycans of bovine aorta, J. Biol. Chem. 270 (1995) 7204–7212.
[39] H. Kitagawa, M. Oyama, K. Masayama, Y. Yamaguchi, K. Sugahara, Structural variations in the glycosaminoglycan–protein linkage region of recombinant decorin expressed in Chinese hamster ovary cells, Glycobiology 7 (1997) 1175–1180.
[40] P.J. Neame, H.U. Choi, L.C. Rosenberg, The primary structure of the core protein of the small, leucine-rich proteoglycan (PG I) from bovine articular cartilage, J. Biol. Chem. 264 (1989) 8653–8661.
[41] F. Cheng, D. Heinegård, A. Malmström, A. Schmidtchen, K. Yoshida, L.Å. Fransson, Pattern of uronosyl epimerization and 4-/6-*O*-sulphation in chondroitin/dermatan sulphate from decorin and biglycan of various bovine tissues, Glycobiology 4 (1994) 685–696.
[42] F.P. Barry, L.C. Rosenberg, J.U. Gaw, T.J. Koob, P.J. Neame, N- and O-linked keratan sulfate on the hyaluronan binding region of aggrecan fron mature and immature bovine cartilage, J. Biol. Chem. 270 (1995) 20516–20524.

Available online at www.sciencedirect.com
SCIENCE DIRECT®
ELSEVIER
International Journal of Pharmaceutics 286 (2004) 1–8
international journal of pharmaceutics
www.elsevier.com/locate/ijpharm

Evaluation of photostability of solid-state nicardipine hydrochloride polymorphs by using Fourier-transformed reflection–absorption infrared spectroscopy – effect of grinding on the photostability of crystal form

Reiko Teraoka*, Makoto Otsuka, Yoshihisa Matsuda

Department of Pharmaceutical Technology, Kobe Pharmaceutical University, Motoyama-Kitamachi 4-19-1, Higashi-Nada, Kobe 658-8558, Japan

Received 7 February 2004; received in revised form 4 July 2004; accepted 17 July 2004
Available online 25 September 2004

Abstract

Photostability and physicochemical properties of nicardipine hydrochloride polymorphs (α- and β-form) were studied by using Fourier-transformed reflection–absorption infrared spectroscopy (FT-IR-RAS) of the tablets, X-ray powder diffraction analysis, differential scanning calorimetry (DSC), and color difference measurement. It was clear from the results of FT-IR-RAS spectra after irradiation that nicardipine hydrochloride in the solid state decomposed to its pyridine derivative when exposed to light. The photostability of the ground samples of two forms was also measured in the same manner. The two crystalline forms of the drug changed to nearly amorphous form after 150 min grinding in a mixer mill. X-ray powder diffraction patterns of those ground samples showed almost halo patterns. The nicardipine hydrochloride content on the surface of the tablet was determined based on the absorbance at 1700 cm^{-1} attributable to the C=O stretch vibration in FT-IR-RAS spectra before and after irradiation by fluorescent lamp (3500 lx). The photodegradation followed apparently the first-order kinetics for any sample. The apparent photodegradation rate constant of β-form was greater than that of α-form. The ground samples decomposed rapidly under the same light irradiation as compared with the intact crystalline forms. The photodegradation rate constant decreased with increase of the heat of fusion.

Keywords: Nicardipine hydrochloride; Photostability; Fourier-transformed reflection–absorption infrared spectroscopy; Crystal form; Solid state

1. Introduction

It is essential to evaluate the photostability of intact drug in preformulation stage of the process of photo-

* Corresponding author. Tel.: +81 78 441 7531; fax: +81 78 441 7532.
E-mail address: teraoka@kobepharma-u.ac.jp (R. Teraoka).

0378-5173/$ – see front matter © 2004 Elsevier B.V. All rights reserved.
doi:10.1016/j.ijpharm.2004.07.026

labile dosage form development. Many investigators have demonstrated the light stability of dihydropyridine analogs in solution. The position of the nitro substitution produced differences in the photostability of the compounds studied and stability studies of the compounds in buffered solutions (pH 7) stored under room light conditions showed that only the ortho-derivative was unstable (Sturm et al., 2001). The effects of the solvent (ethanol, acetone, dichloromethane), drug concentration and radiation wavelength on the lacidipine photostability were evaluated and the cis-isomer and a photocyclic isomer proved to be the main photodegradation products (De Filippis et al., 2002). Photodegradation of nilvadipine was carried out under the conditions recommended in the first version of the document issued by the International Conference on Harmonization (ICH), currently in force in the studies of photochemical stability of drugs (Augustyniak et al., 2001; Mielcarek et al., 2000). In addition, there have been several reports (Akimoto et al., 1988; Binda and Dondi, 1981; Ebel et al., 1978; Thoma and Klimek, 1985) dealing with the photodegradation of nifedipine in solution. However, there are few reports (De Villiers et al., 1992; Matsuda et al., 1994; Matsuda and Tatsumi, 1990; Qin and Frech, 2001; Teraoka et al., 1999) on the effect of crystal and amorphous forms of drug photostability because the topochemical photodegradation in the solid state was influenced by the particle size and, consequently, it is very difficult to establish the reproducible experimental conditions.

Nicardipine hydrochloride (2-(*N*-benzyl-*N*-methylamino) ethyl methyl (RS)-1, 4-dihydro-2,6-dimethyl-4-(3-nitrophenyl)-3, 5-pyridinedicarboxylate monohydrochloride) is an effective calcium antagonist and has been widely used for the treatment of coronary heart disease. The drug is commercially available in injections, tablets, and powders. Although its stability in injectable solutions have been reported (Baaske et al., 1996; Bonferoni, 1992), the photostability in the solid state has not been established to date.

Nicardipine hydrochloride was isolated by Iwatani et al. (1979) in two crystalline forms and the two crystalline forms were characterized by Yan and Giunchedi (1990). Qin and Frech (2001) reported that the photodegradation rate of the amorphous MK-912 was approximately 40 times faster than that of the crystalline MK-912 under the photostability test conditions of the ICH guidelines.

Grinding is often carried out to reduce the particle size of the intact drug. However, not only desired changes in physical properties such as specific surface area and shape, but also changes in physicochemical properties such as catalytic activity can take place during grinding, and consequently polymorphic transformation or conversion to amorphous form may occur. Kitamura et al. (1989) reported that the ground cefixime crystals showed an increase in the apparent discoloration rate constant with the increase in the grinding time.

The photodegradation of drug in the solid state is a topochemical reaction, and therefore, it is not appropriate to evaluate the decomposition ratio by conventional analytical methods such as HPLC, UV, and IR spectroscopy. Fourier-transform infrared reflection–absorption spectroscopy (FT-IR-RAS) allows pure materials to be analyzed without addition of KBr (Golden, 1985). Recently, photostability of carbamazepine polymorphs (Matsuda et al., 1994) and nifedipine (Teraoka et al., 1999) was investigated by using FT-IR-RAS. Therefore, we used FT-IR-RAS to measure pure materials using nicardipine hydrochloride tablets. The purpose of the present study was to evaluate the photodegradation of crystalline and ground nicardipine hydrochloride by using a simple and fast FT-IR-RAS method for quantitative determination of the drug.

2. Materials and methods

2.1. Materials

Bulk nicardipine hydrochloride powder (α- and β-forms) was kindly supplied Yamanouchi Ltd. Japan and those samples were used without purification. The commercial solvents for HPLC analysis were used without further purification.

2.2. Mechanical treatment

The drug powder was ground for 150 min in a 10 mL agate vessel by vibrating-type mixer mill (model MM2, Retsch Co., Germany), containing agate ball (the diameter and number of ball was 12 mm × 1) at 25 °C.

2.3. Preparation of sample pellets

The accurately weighed intact and ground nicardipine hydrochloride powders of two crystal forms

(500 mg) were compressed using an accurate compression/tension testing machine (Autograph model IS-5000, Shimadzu Co., Kyoto, Japan) equipped with flat-faced punches and a cylindrical die (20 mm i.d.) set at a compression speed of 15 mm/min at 9.8 kPa, and then the pellet of ca. 1.5 mm in thickness was prepared. The variation in thickness of these pellets was negligible among two forms and amorphous forms, thus suggesting that the surface morphology of these pellets was almost the same.

2.4. Irradiation test

Sample pellets were stored in a light-irradiation tester (Light-Tron LT-120, Nagano Science Co., Takatsuki, Japan) equipped with a white fluorescent lamp (rapid-start type 20 W). The illuminance was set at 3500 lx. The irradiation tests were carried out at 25 °C and 0% relative humidity.

2.5. X-ray powder diffraction analysis

X-ray powder diffraction patterns were measured by an X-ray diffractometer (XD-3A, Shimadzu Co., Kyoto, Japan) at room temperature. The operating conditions were as follows: Target, Cu; filter, Ni; voltage, 30 kV; current, 15 mA; receiving slit, 0.1 mm; time constant, 1 s; scanning speed, 4° 2θ/min.

2.6. FT-IR-RAS measurement

FT-IR spectra of the sample pellets were obtained by FT-IR-RAS on an FT-IR spectrometer (model FT-IR 1600, Perkin Elmer Co., Yokohama, Japan) and modified by using the Kramers-Krönig equation. The spectral data were not transformed by the normalized function.

2.7. Colorimetric measurement

The surface color of the compressed sample pellet was measured with an integrating sphere-type color difference meter (model ND-300A, Nippon Denshoku Co., Tokyo, Japan) after the designated irradiation times. The color difference (ΔE) before and after irradiation was calculated to evaluate the degree of discoloration (Matsuda et al., 1989). All values were the averages of two measurements.

2.8. Photodiode array procedures for nicardipine hydrochloride

The photodiode array for nicardipine hydrochloride after storage was carried out by an HPLC system (Waters) equipped with a photodiode array detector (Waters, model 991J); the prepacked column (LiChrospher 100 CN (5 μm), 15 cm × 4.0 mm, Merck, Japan) was operated at room temperature at a flow rate of 0.7 mL/min. The mobile phase was composed of a mixture of 0.01 M sodium phosphate buffer (pH 6.1) and acetonitrile (1:1 v:v). After irradiation, the surface of the pellet was scraped off and dissolved in methanol. Subsequently the solution was analyzed by the above HPLC system.

2.9. Thermal analysis

The thermograms of the two crystal forms and the ground powders were recorded on a differential scanning calorimetry (DSC) (model 3100, Mac Science Co., Tokyo, Japan). The operating conditions in the open-pan system were as follows: sample weight, 5 mg; heating rate, 180 °C/min; N_2 gas flow rate, 50 mL/min.

3. Results and discussion

3.1. Grinding of α- and β-forms of nicardipine hydrochloride

Fig. 1 shows the X-ray powder diffraction patterns of the intact crystals of nicardipine hydrochloride and 150 min ground samples. These crystals exhibit characteristic patterns and the X-ray powder diffraction patterns of α- and β-forms were confirmed to be the same as those reported by Yan and Giunchedi (1990). The diffraction peak intensities of two forms decreased after grinding and X-ray powder diffraction patterns of the two forms ground for 150 min showed almost halo patterns. This suggests that most of α and β-forms converted into amorphous state.

The thermal profiles of nicardipine hydrochloride modifications are shown in Fig. 2. The α- and β-forms had an endothermic peak due to fusion at 188.7 °C and 171.1 °C, respectively. After 150 min of grinding in mixer mill, the temperature of both endothermic peaks became lower and α-form showed an exothermic peak

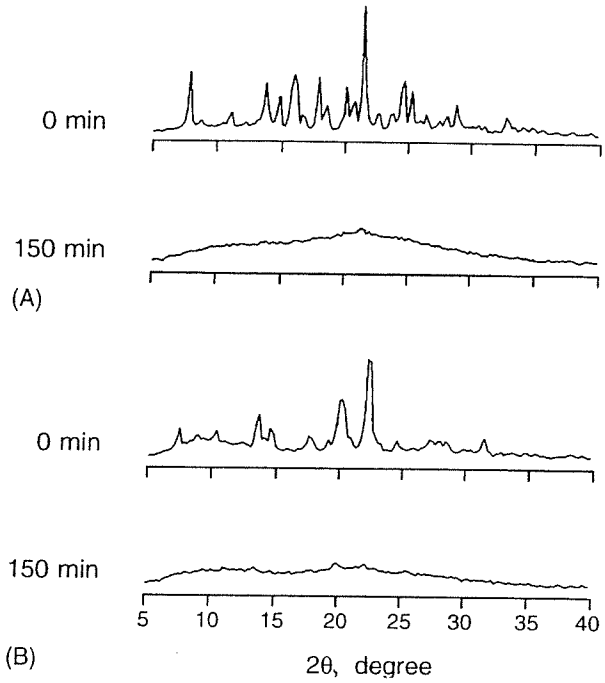

Fig. 1. Changes in X-ray powder diffraction patterns of nicardipine hydrochloride polymorphs after grinding: (A) α-form; (B) β-form.

at 150 °C due to crystallization, and then an endothermic peak at 181.2 °C due to fusion. On the other hand, the ground β-form sample showed no exothermic peak and exhibited a weak endothermic peak at 163.8 °C due to fusion, suggesting that the ground β-form was higher amorphism compared with the ground α-form. That is to say, the ground β-form has a greater degree of disorder of the molecular arrangement. X-ray powder diffraction profiles of both ground powders had no change and showed almost halo patterns when these powders were stored at 25° in a desiccator with phosphorus pentoxide for two weeks. This result suggests that these amorphous powders were stable and crystallization did not occur under low humidity. Therefore, light stability test was performed in the closed box which put transparent quartz glass in the window and was maintained at low humidity with phosphorus pentoxide.

3.2. Photodegradation product

Fig. 3 shows the chromatograms resulting from the HPLC analysis of the powder scraped from tablet surface after irradiation under the white fluorescent lamp at 3500 lx. The two peaks were detected at 260 nm after irradiation, and a new peak at 4.2 min appeared as a result of photochemical reaction in addition to nicardipine hydrochloride at 5.3 min. The UV spectra corresponding to these peaks were obtained by photodiode array technique (Fig. 3) and peaks a and b exhibited λ_{max} of the UV spectra at 237 nm and between 250 and 290 nm, respectively. Photostability of nicardipine hydrochloride solution under both UV and daylight conditions was reported by Bonferoni et al. (1992). They reported that nicardipine hydrochloride was light-sensitive and the drug gave rise to the pyridine derivative by the photodegradation. As compared with their results of UV spectra obtained by photodiode array method, the peak b indicated to be the pyridine derivative of nicardipine hydrochloride. It was clear that nicardipine hydrochloride was degraded in the solid state as well as in the solution under white fluorescent lamp.

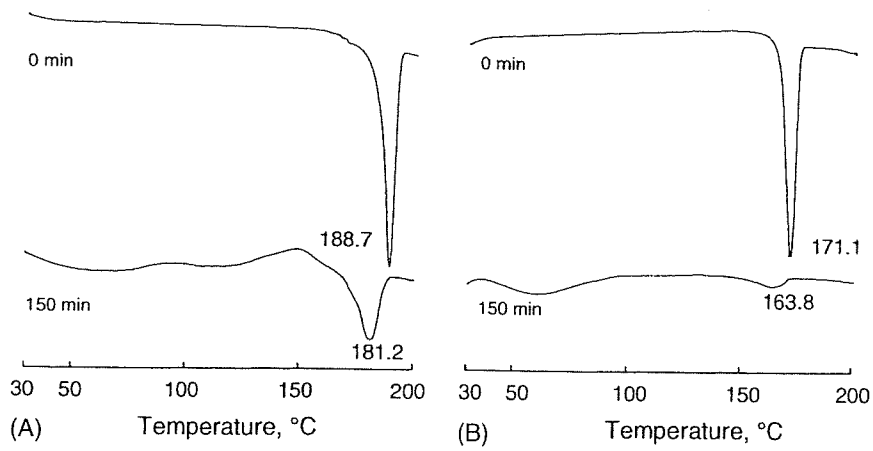

Fig. 2. Changes in DSC curves of nicardipine hydrochloride polymorphs after grinding: (A) α-form; (B) β-form.